The Use of ERS-1 SAR Data in Snow Melt Monitoring

Jarkko T. Koskinen, *Student Member, IEEE,* Jouni T. Pulliainen, *Member, IEEE,* and Martti T. Hallikainen, *Fellow, IEEE*

***Abstract*—ERS-1 SAR data, airborne data and *in situ* snow data were acquired for the Sodankylä test site in northern Finland for the winters of 1991–1992 and 1992–1993. The test area consists of sparsely forested areas (pine, mixed forests, and mires) and open areas (bogs, lakes, clear-cut areas, and urban area).**

A set of multitemporal ERS-1 SAR images covering the two winters have been analyzed and the results have been compared with *in situ* surveys and a digital land-use map. The results indicate that even in the presence of forest canopies 1) wet snow can be distinguished from other soil/snow conditions (dry snow and bare ground), and 2) snow melt maps can be derived from SAR images. Snow-melt maps indicate areas fully covered with wet snow, partly melted areas and snow-free areas.

I. Introduction

MANY environmental processes are strongly affected by the presence of snow. Knowing the amount and distribution of snow helps to improve weather forecasts, to predict water supply for hydropower stations, to anticipate flooding, to forecast crop yields and to estimate freeze damage [1].

Remote sensing has been used successfully for snow monitoring. Optical and near infrared sensors can discriminate snow-cover from bare ground and remote sensing data have been used as input to snow runoff models for near real time and seasonal runoff forecast [2], [3]. Passive microwave sensors have a long history in snow monitoring. Several investigations have demonstrated the capability of multifrequency microwave radiometer systems to locally map snow extent, snow depth, and snow water equivalent [4], [5]. Experiments with Seasat and ERS-1 SAR data have demonstrated the capability of spaceborne SAR to distinguish wet snow from bare ground [6]–[8] and estimate snow liquid water content [9].

In the framework of ESA ERS-1 Announcement of Opportunity program, we received ERS-1 SAR data from the Sodankylä test site for the winters of 1991–1992 and 1992–1993. Additionally, we conducted scatterometer measurements in the test site using our 8-channel HUTSCAT system [10]. The two data sets covered the four basic soil/snow conditions: frozen and thawed snow-free terrain and dry and wet snow-cover [7].

The final goal of our studies on remote sensing of snow is to develop a method to monitor the snow-cover by using multisensor data (i.e., ground-based and satellite-based measurements and precipitation and runoff models). In this project the following two topics were examined [1]:

1) *Capability of ERS-1 SAR to identify snow-covered ground and melting snow*. Snow-free ground may be either thawed or frozen and the snow-cover may be either wet or dry. The backscattering properties of the snow-soil system for each case were explored. The SAR data may be able to make a significant contribution to satellite observations of snow by bridging the period between the on-set and end of snow melt. Microwave radiometers can be used to retrieve the water equivalent of dry snow, but they cannot be used to distinguish between wet snow and wet ground during the melting period [7].
2) *Effect of vegetation to snow mapping*. The results from the test site were analyzed for all available vegetation and surface types in order to determine the backscattering contribution from each land-use category. This is important for snow mapping by satellite-borne SAR. In particular, the effect of different forest canopies versus open areas to the backscattering coefficient was investigated.

II. Snow in Finland

The first snow-cover settles over Finland during October–November and, normally, after 15 to 50 days, the seasonal snow-cover takes over Finland. The annual maximum water equivalents in southern Finland occur from February to March and in northern Finland from March to May and the mean values vary from 100 to 200 mm [11]. The melting of snow is the most important physical process in the formation of spring floods in Finland. The water equivalent at the beginning of melt is usually six to ten times larger than the total precipitation during the snow melt period. Only occasionally does precipitation give an essential contribution to the potential of the spring flood. The average date of the beginning of the maximum five-day water yield varies from March (west coast) to May (northern Finland). The daily mean maximum of water yield may vary from 59 l s^{-1} km^{-2} to 217 l s^{-1} km^{-2} at different basins [12]. Due to the fact that about 65% of land area in Finland is covered by forests [13], a single snow edge normally does not exist. Usually the snow melt starts around trees forming circular snow-free plots. Gradually these plots get bigger and finally they reach each other. Therefore, in

Manuscript received June 18, 1996; revised November 29, 1996.

The authors are with the Helsinki University of Technology, Laboratory of Space Technology, 02150 Espoo, Finland (e-mail: jarkko@avasun.hut.fi).

Publisher Item Identifier S 0196-2892(97)03669-3.

forested areas snow melt can be monitored by estimating the relative fractions of snow-free area and snow-covered area.

The Finnish Environment Agency publishes a map of the snow water equivalent in Finland twice a month [14]. The map (Fig. 1) is based on results from ground-based measurements employing a network of snow courses. The absolute standard error of the water equivalent in the map for a basin with an area of 1000 km^2 is typically between five and 15 mm in the accumulation period. For a large river basin exceeding 10 000 km^2 in area, the corresponding error is 5 to 10 mm. During the melting period, the absolute standard error is higher, ranging from 10 to 20 mm [12].

III. Test Site and Ground Truth

Our test site is located in Sodankylä (center latitude = 67.41 N, center longitude = 26.58 E) and its size is 40 km × 40 km [15].

A digital land-use map of the Sodankylä test site was obtained from the National Board of Survey. The spatial resolution of the map is 25 m × 25 m. The map is based on classification made by employing TM and SPOT images and a thematic map. The accuracy of the classification varies from 65 to 100%. For the forest classes the stem volume is classified into 50 m^3/ha intervals [16]. A total of 23 land-use categories is used to describe our test site (Table I). The water category consists of small lakes and rivers. The urban area class is solely the commercial center of Sodankylä. The forest areas consist of pine and mixed types on mineral soil, where the stem volume per hectare is usually low. The other major soil type of forest class is mire (peat land) and it is usually densely covered with small birch or pine trees. The open bogs are large open areas with several pond-like openings. The vegetation in these areas consists of brush on peat land.

In order to increase the reliability of stem volume values in the land-use map, a digital stem volume map was obtained from the Finnish Forest Research Institute. The stem volume map has been produced using ground-based methods and satellite imagery as a part of the Seventh National Forest Inventory. The stem volume is classified into 2 m^3/ha intervals. The spatial resolution of the map is 25 m × 25 m [17].

A total of 19 test lines was selected within the test site for airborne and ground-based measurements (Table I). The total length of the test lines is over 9 km. The properties of the forest canopies along the test lines were measured, including the tree type, height, and stem volume [18]. Extensive field measurements were conducted along the test lines during the airborne campaigns. The measured parameters include the snow extent, physical parameters of snow cover and underlying soil and, additionally, weather data [18]. This snow and weather data was used to select suitable images for the study.

IV. ERS-1 SAR Data Set

The data set used in this study consists of 21 ERS-1 SAR images. The images are listed in Table II with available snow data (by National Board of Waters and the Environment) and weather data (by Meteorological Institute). The original SAR images, delivered in PRI format, were rectified and geocoded by the Technical Research Center of Finland (VTT). This was performed using the geocoding algorithm with a digital elevation model developed by Rauste [19]. The algorithm corrects the errors caused by topography but no radiometric corrections are made to the images. There are no major elevation differences nor steep slopes in the test site. The preprocessed images delivered from VTT included three channels for every acquired SAR image and the pixel size was undersampled to 25 m × 25 m. The first channel is the rectified SAR image. The second channel represents the local angle of incidence for every pixel and the third channel shows the size of the pixel in percent where 100% refers to the pixel size of 25 m × 25 m.

TABLE I
Land Use Classification in the Sodankylä Test Site, Occurrence of Each Land-Use Class on Airborne Test Lines, and Relative Coverage in the ERS-1 Test Site

No.	Land-use class	Number of airborne test line	Relative coverage in ERS-1 test area (%)
1	Water	5,10	2.3
2	Agricultural land	18c	1.2
3	Gravel	4,11	0.5
4	Urban area	6	0.2
5	Clear-cut	1a,17,18a	8.0
6	Pine (0-50 m^3/ha)	1b,14,18b	16.4
7	Pine (50-100 m^3/ha)	3b,7b,12,15	19.9
8	Pine (100-150 m^3/ha)	1c,19	5.9
9	Pine (150-200 m^3/ha)	-	2.0
10	Pine (200- m^3/ha)	-	1.8
11	Deciduous (0-50 m^3/ha)	-	8.7
12	Deciduous (50-100 m^3/ha)	-	5.5
13	Deciduous (100- m^3/ha)	-	1.5
14	Mixed (0-50 m^3/ha)	-	0.2
15	Mixed (50-100 m^3/ha)	7a	1.1
16	Mixed (100- m^3/ha)	-	0.4
17	Open bog	2	13.9
18	Forested bog	8,9,13,16	8.8
19	Bare mountain top	-	1.7
Total		19 lines	100%

V. Effect of Snow-Cover and Vegetation

All 21 SAR images used in the study were divided into four categories (wet snow, dry snow, thawed snow-free ground, frozen snow-free ground) by using weather information and snow maps. The means and the standard deviations (the calculation is made using 25 m × 25 m pixel size), of the backscattering coefficients were calculated for each land-use class in different snow conditions [20]. Fig. 2(a) shows that the mean values for thawed snow-free ground and frozen snow-free ground are practically the same. They are about 1 dB higher than those for dry snow, depending on land-cover type. Only the mean values for wet snow are clearly different from those for other categories. This suggests that the potential of ERS-1 SAR in discriminating snow/soil categories is limited to classifying wet snow. The difference between the mean value

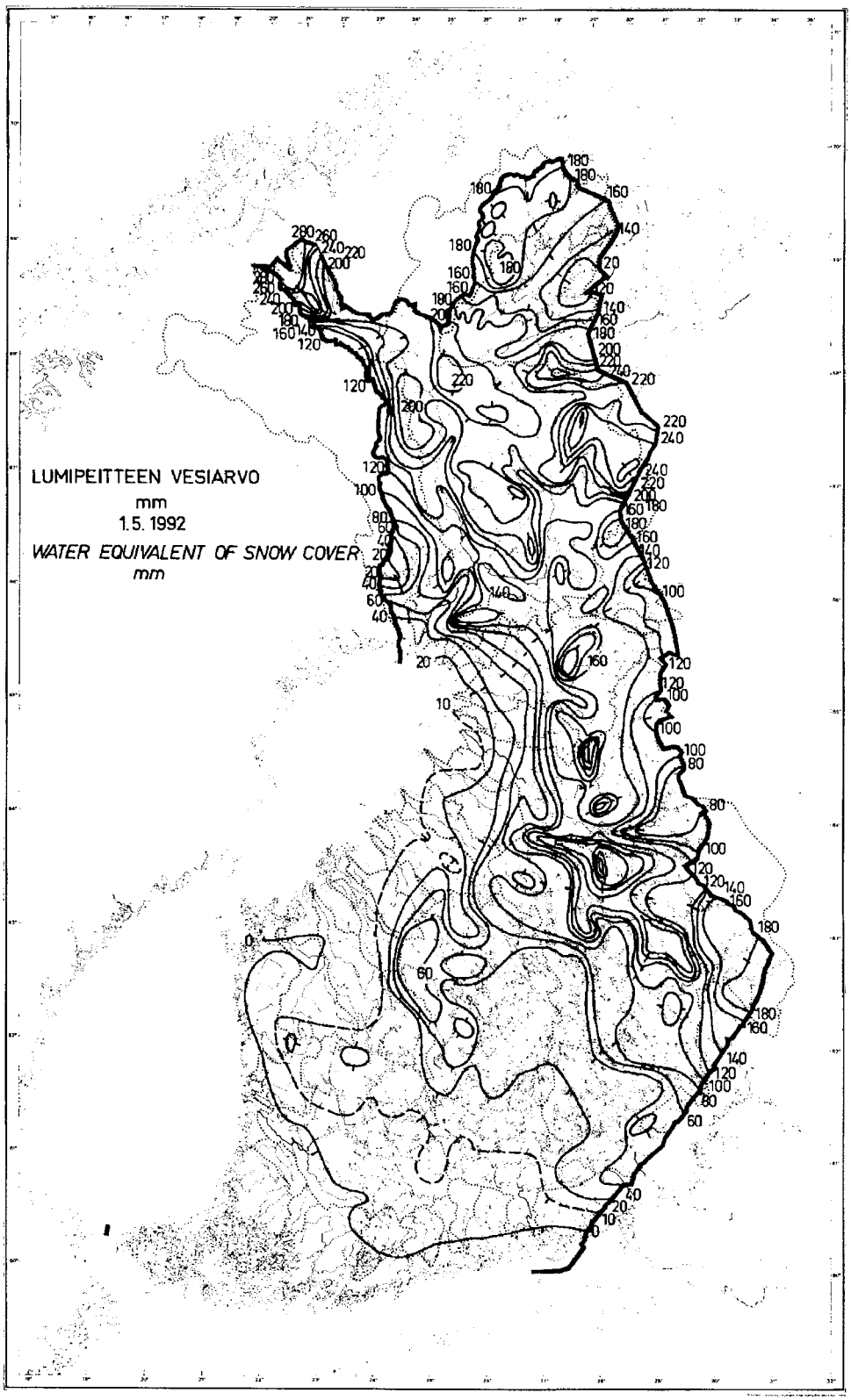

Fig. 1. Snow water equivalent map of Finland for May 1, 1992 [14].

of the backscattering coefficients for wet snow and the other categories is about 3 dB for open areas. The difference decreases with increasing biomass in the test site. Fig. 2(b) shows the standard deviation for the three categories. For the densely forested pine categories the standard deviation is practically independent of snow/soil condition. This is in agreement with recent results [21]. A standard deviation of 2–2.5 dB means that the capability of ERS-1 SAR to discriminate wet snow from other snow/soil categories may be limited, depending on land-cover category and measurement condition.

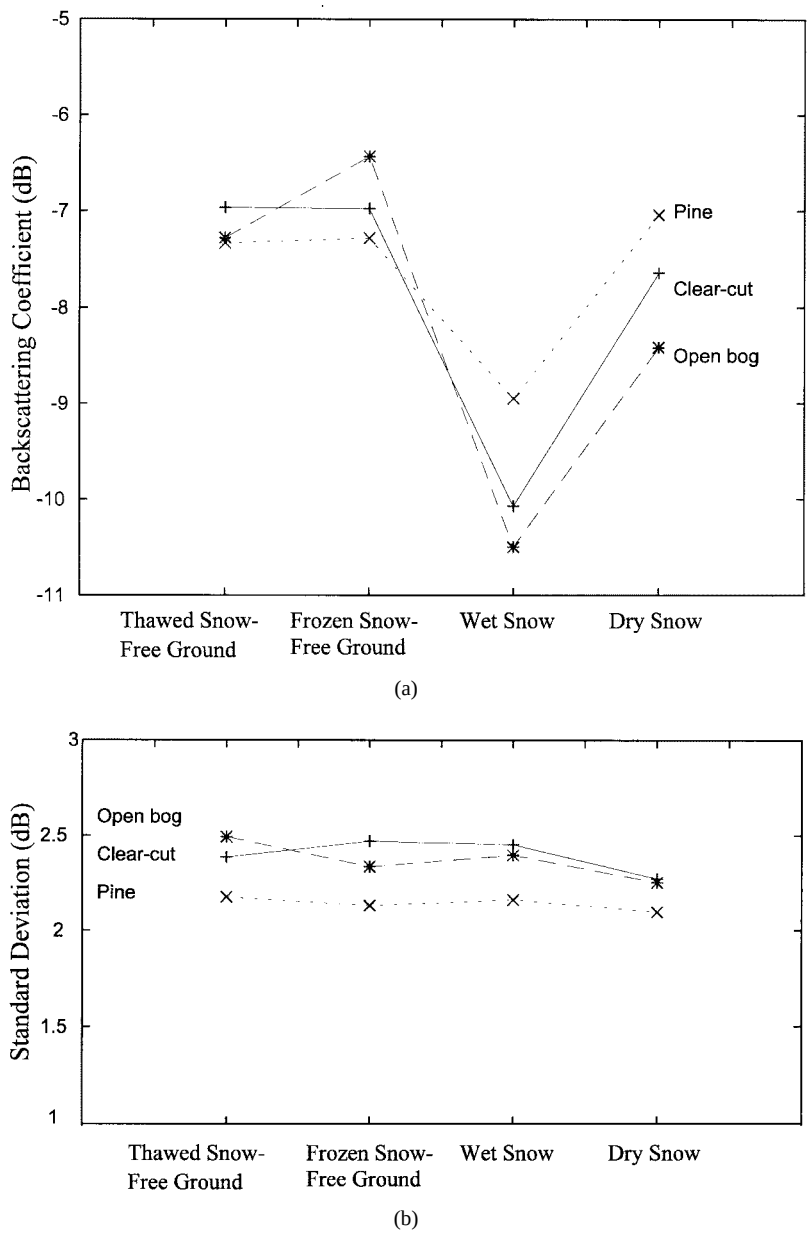

Fig. 2. (a) ERS-1 SAR derived average backscattering coefficients and (b) standard deviations of backscattering coefficients for clear-cut, open bog and forest areas in different snow conditions. The results are based on 21 images (see Table II).

The dependence of the accuracy of wet snow classification on the area size was tested by dividing the total test area (1600 km^2) into smaller regions. Three land-use classes were selected to be used in this study: open bog, clear-cut and pine 50–100 m^3/ha. The Maximum Likelihood classifier (ML) was employed in the classification [22]. By employing the whole test site the classification accuracy was always higher than 90% for every land-use class. When the sample area was decreased to 100 km^2 the classification accuracy varied from 85 to 90%. For a 1 km^2 size the accuracy of wet snow classification was about 80% and when size was further reduced the accuracy decreased rapidly because some of the sample areas had few independent samples for each land-use class and so the effect of speckle began to dominate. Also the local variation in the land-use class-wise mean values increased deviation when a sample from a certain land-use class was compared to a sample of the same land-use class taken from a different part of the test site.

The effect of vegetation was analyzed by comparing the results from a semi-empirical model developed by Pulliainen [23] with the ERS-1 SAR based means of the backscattering coefficients obtained for different stem volume classes. The backscattering coefficient of forest land σ^o can be written as

$$\sigma^o = \sigma_v^o + t^2\sigma_g^o, \tag{1}$$

where

- σ_v^o backscattering coefficient contribution from the forest canopy;
- t forest canopy transmissivity;
- σ_g^o backscattering coefficient of the ground, including the trunk-ground reflection.

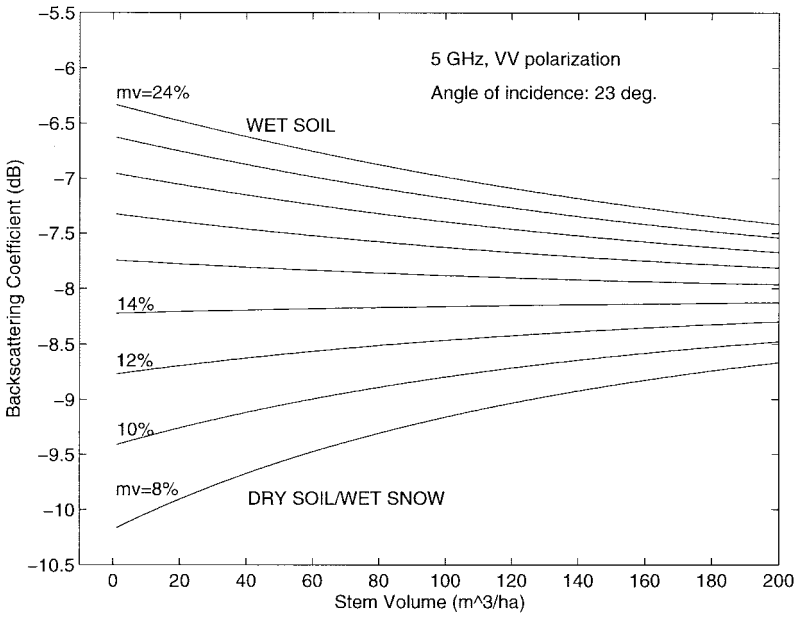

Fig. 3. Modeled behavior of σ^0 at 5.3 GHz, VV polarization, 23° incidence angle as a function of stem volume with a varying volumetric value of soil moisture (2%-unit intervals). The results for low soil moisture values resemble those for wet snow (see text).

TABLE II
ACQUIRED SAR IMAGES AND RESPECTIVE WEATHER AND SNOW CONDITIONS. INFORMATION ON SAR IMAGES USED FOR DETECTING SNOW MELT IS IN BOLD

Date	Precipitation (mm)	Temperature min/max (°C)	Snow water equivalent (mm)	Ground condition
Feb. 2, 1991	3.7	1.2 / 3.9	0	wet ground
Oct. 23, 1991	0.1	-4.8 / -2.0	0	frozen ground
Apr. 15, 1992	0	-13.6 / 2.2	180	dry snow
May 1, 1992	**2.2**	**-1.3 / 0.4**	**180**	**wet snow**
May 20, 1992	**0**	**0.6 / 8.4**	**0 to 10**	**wet snow**
May 29, 1992	0	7.8 / 25.2	0	wet ground
Jun. 24, 1992	10.0*	4.6 / 15.2	0	wet ground - dry canopy
Jul. 29, 1992	30	10.4 / 17.3	0	wet ground
Sep. 18, 1992	17	3.5 / 9.4	0	wet ground
Nov. 11, 1992	1.8	-2.0 / 2.7	10 to 20	wet snow
Dec. 16, 1992	3.2	-7.7 / -4.0	80	dry snow
Jan. 20, 1993	1.4	-24.2 / -8.0	140	dry snow
Feb. 24, 1993	0.2	-15.2 / -10.3	200	dry snow
Mar. 31, 1993	1.9	-7.0 / 0.0	220	dry snow
Apr. 16, 1993	4.5	-8.5 / 1.0	200	dry snow
May 5, 1993	**0**	**0.6 / 4.6**	**0 to 120**	**wet snow**
Jun. 2, 1993	**15**	**8.6 / 16.2**	**0**	**wet ground**
Jun. 9, 1993	**6.9****	**1.6 / 5.6**	**0**	**wet ground**
Jun. 18, 1993	2.5	5.1 / 19.6	0	wet ground
Jun. 25, 1993	0	2.9 / 17.0	0	dry ground
Jun. 28, 1993	0	8.4 / 18.0	0	dry ground

*) 3 days earlier **) previous day

When a forest canopy is measured with a high-resolution ranging scatterometer, the two backscattering contributions of (1) can be distinguished from each other. Moreover, the canopy transmissivity as a function of forest stem volume can be determined by obtaining $t^2\sigma_g^o$ (ground backscattering contribution) for areas with various stem volumes. The semi-empirical model used here was developed applying this approach for a large forest area and using HUTSCAT data from the Teijo test area [24]. The effects of soil and canopy moisture variations have been incorporated into the modeling approach using well-known empirical models [25]–[27]. The seasonal and diurnal changes in σ^o are caused by the changes in the vegetation and soil moisture, freeze/thaw effects, seasonal defoliation, and snow cover.

The forest canopy backscattering contribution can be written in terms of the stem volume as [24]

$$\sigma_v^o = \frac{C}{-2a_1}[1 - e^{2a_1 v}] \tag{2}$$

where

C empirical coefficient for canopy backscatter [ha/m^3];
a_1 empirical coefficient for canopy extinction [ha/m^3];
v forest stem volume [m^3/ha].

The values obtained for the above constants in dry summer day-time conditions for 5.4 GHz, VV polarization, 23° angle of incidence (corresponding to ERS-1 SAR characteristics) are: $C = 9.68\times.10^{-4}$ and $a_1 = -2.78\times10^{-3}$ [24]. In summer conditions the extinction coefficient a_1 can be assumed to be linearly related to the volumetric canopy moisture, while the change of C can be assumed to be related to the square of the change in volumetric moisture [26]. This formula applies also to winter responses; then a_1 and C are not dependent on the moisture but, rather, on the dielectric constant of the frozen wood. The results from the semi-empirical model are shown in Fig. 3.

Fig. 3 shows that the radar response to the stem volume is highly dependent on the soil dielectric constant, especially for low values of the stem volume. The slope of σ^o versus

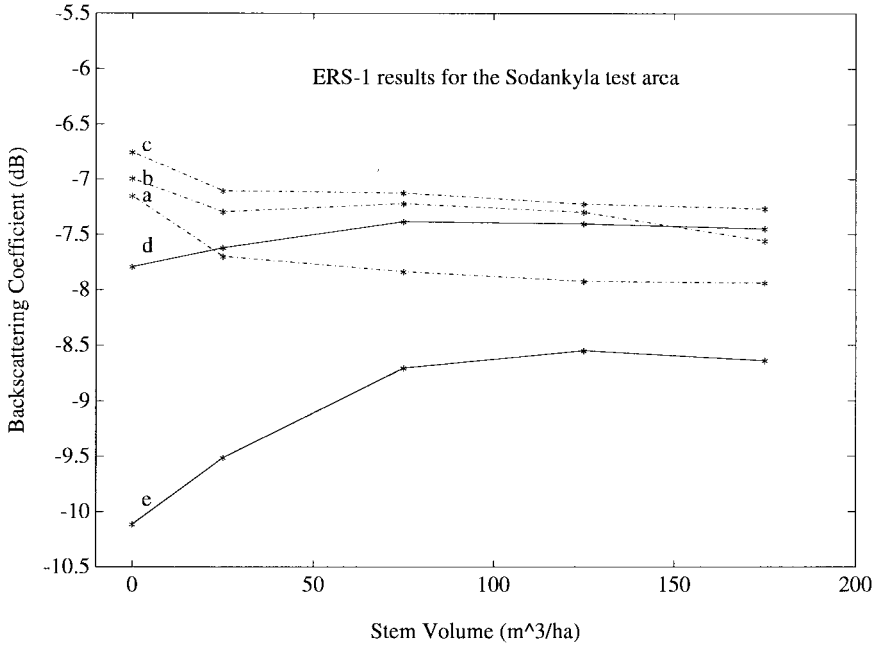

Fig. 4. ERS-1 SAR derived mean values for the backscattering coefficient in the Sodankylä test site. The results are presented for clear-cut areas and for the following stem volume categories: 0–50, 50–100, 100–150, and 150–200. (a)–(c) Summer conditions, (d) dry snow, (e) wet snow.

stem volume varies from positive to negative depending on the soil conditions, and the standard deviation of σ^o decreases when stem volume increases. Freezing of the soil or presence of wet snow cover reduces dramatically σ_g^o contribution and, therefore, frozen soil and wet snow behave in this regard like dry soil. The HUTSCAT experiments conducted in winter show that the canopy backscattering contribution σ_v^o does not change that much. This is due to the fact that backscattering contribution from the vegetation canopy is dominated by volume scattering. Hence, as the freezing of vegetation canopy decreases the volume backscattering coefficient, the canopy transmissivity increases concurrently causing the canopy σ_v^o-contribution to remain nearly . This has also been observed in radar experiments [23] (e.g., winter-time HUTSCAT experiments conducted in Sodankylä area).

ERS-1 SAR data for the Sodankylä test site were used to analyze the effects of snow-cover to the backscattering coefficient. Fig. 4 presents the ERS-1 SAR results as a function of stem volume in winter conditions (for dry snow cover and wet snow-cover) and, for comparison, in summer conditions. The results confirm that radar backscattering for snow-covered terrain behaves like that for snow-free ground with low soil moisture. The results also show that the response to the stem volume is the highest with the presence of wet snow-cover. This phenomenon occurs obviously due to the high signal attenuation caused by the wet snow and due to the low level of backscatter from the smooth air-snow boundary. The response to the stem volume saturates around 150 m^3/ha, suggesting that the radar backscatter for stem volumes above 150 m^3/ha comes from the forest canopy only.

VI. Detection of Snow Melt

Detection of snow melt was investigated by observing the differences between SAR images acquired at the beginning, during and after the melt period. A similar approach has been used before in high mountain areas in Switzerland where images taken during the melt period were compared either to preceding dry snow or succeeding open ground reference image [28]. The difference between these approaches is that we used two reference images, which represent the beginning of melt period when the whole area is covered by wet snow and post-melt period when all of the snow is melted. Hence, we are able to do a more exact approximation over the whole snow melt period.

Due to the ERS-1 orbit configuration we could not have all images from the same melt period. Hence, we needed to use images from the melt periods in 1992 and 1993. We compared these periods in order to verify the feasibility of this approach. Fig. 5 shows a comparison of the average temperature and snow water equivalent for the two melt periods. It is evident from Fig. 5 that the conditions in 1992 and 1993 were very close to each other. This justifies our approach.

The data set used in the snow melt study consists of five images which were acquired during the springs of 1992 and 1993 (shown in Table II in bold). The first image was acquired on May 1, 1992, when the air temperature was well above 0 °C and the water equivalent of snow in the test area was about 180 mm. The second image was acquired on May 5, 1993 when the snow-cover had melted substantially so that the water equivalent varied from 0 to 120 mm. Snow in some fields, clear-cuts and open bogs had melted but most of the test area was covered by snow. According to the visual estimates made by an experienced hydrologist the snow-cover percentage varied from 99 to 30 depending on the test line (Table III). The estimates are based on video imagery covering all the test lines. The third image represents the final step of the melting period (May 20, 1992) when the snow water equivalent varied from 0 to 10 mm. Almost all of the snow had

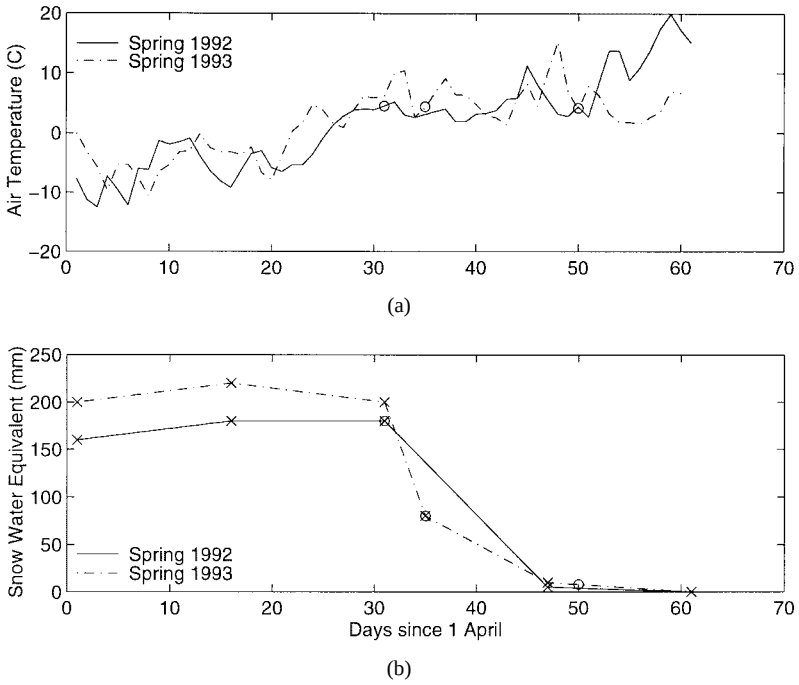

Fig. 5. Comparison of (a) *in situ* air temperature and (b) snow water equivalent during the springs of 1992 and 1993. Circles denote SAR images used in the analysis.

melted in open areas and bogs, but some snow still existed in forested areas. The fourth and fifth image were acquired after the melt season (June 2, 1993 and June 9, 1993) and no snow existed at that time. The ground was wet in the whole test area. Although the weather and snow data were collected from the test lines, the results are considered to be representative for the whole 40 km $\times$ 40 km test area.

Fig. 6 shows the behavior of the backscattering coefficient for clear-cut areas and various pine categories during the melt seasons of 1992 and 1993. Based on the behavior of the backscattering coefficient in Fig. 1, the increase of σ^0 in Fig. 6 is proportional to the fraction of snow-free terrain in the test site. On May 1, 1992 the test area is covered with a deep wet snow layer. The backscattering from wet snow (σ_g^0) is very low and therefore the backscatter contribution from the ground behaves similarly to that from very dry ground (see Fig. 3). By May 5, 1993 snow melt has occurred mostly in clear-cut areas and in sparsely forested areas. The percentage of snow-free ground in Table III supports the interpretation. When part of the snow has melted resulting a mosaic of snow-free and wet snow-covered areas, the level of σ_g^0 increases and, consequently σ^0 increases significantly, see (1) and Fig. 3. At the time when the second image was acquired the forest canopy moisture may have been lower than in the first image. Therefore, the backscattering coefficient for the highest stem volume class is lower than in the first image. On May 20, 1992 the snow melt has progressed in all stem volume classes. The highest changes occur in clear-cut areas and sparsely forested areas where almost all of the snow has melted and the ground is wet. Hence, radar backscatter is high in agreement with the model predictions for the soil moisture of 16–18% (see Fig. 3). Fig. 6 confirms the well-known fact that when open areas and sparsely forested areas are practically free of snow, there is still plenty of snow in densely forested areas.

TABLE III
OBSERVED PERCENTAGE OF SNOW-FREE GROUND ON AIRBORNE TEST LINES ON MAY 5, 1993

Test line	Land-use class	Snow-free ground (%)
1a	Clear-cut	31
1b	Pine (0-50 m^3/ha)	31
1c	Pine (100-150 m^3/ha)	31
2	Open bog	-
3	Pine (50-100 m^3/ha)	5
4	Gravel	76
5	River Kitinen	-
6	Urban area	-
7a	Mixed (50-100 m^3/ha)	11
7b	Pine (50-100 m^3/ha)	11
8	Forested bog	43
9	Forested bog	12
10	Lake Orajärvi	18
11	Gravel	-
12	Pine (50-100 m^3/ha)	2
13	Forested bog	8
14	Pine (0-50 m^3/ha)	18
15	Pine (50-100 m^3/ha)	2
16	Forested bog	24
17	Clear-cut	70
18a	Clear-cut	9
18b	Pine (0-50 m^3/ha)	9
18c	Agricultural land	9
19	Pine (100-150 m^3/ha)	1

We can estimate the relative fraction of snow-free ground from a SAR image by comparing it with two other images, one acquired at the beginning of the melt period (wet snow)

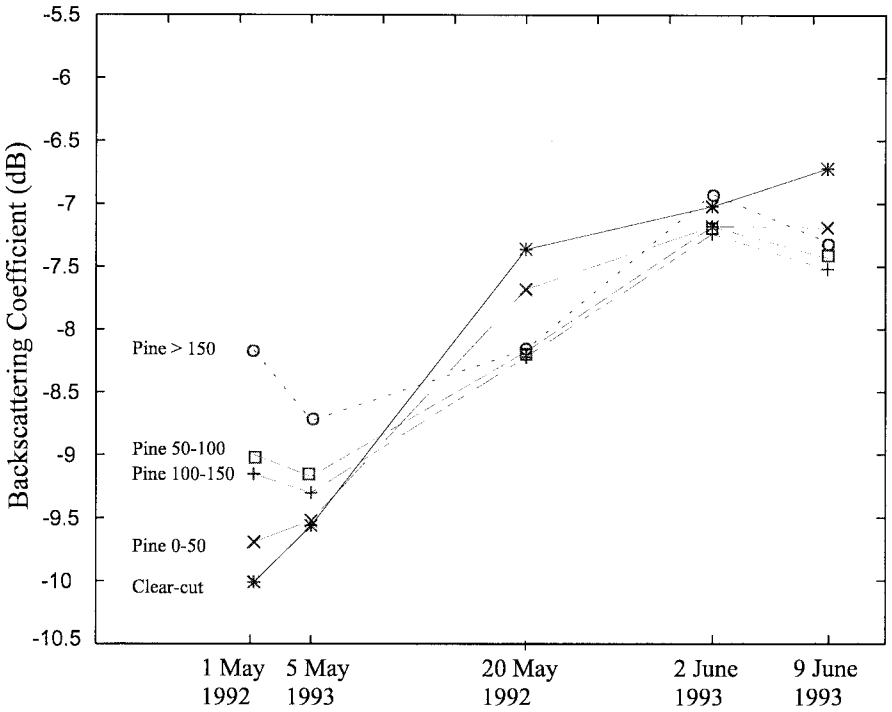

Fig. 6. Behavior of σ^0 during snow melt for different vegetation classes. Results are based on the following SAR images: (a) May 1, 1992, SWE 180 mm, wet snow; (b) May 1, 1992, SWE 0–120 mm, wet snow; (c) May 20, 1993, SWE 0–10 mm, wet snow; (d) June 2, 1993, wet ground; and (e) June 9, 1993, wet ground.

and the other acquired after the melt period (thawed snow-free ground). By conducting a pixel-wise comparison between the three images, the following equation for the relative fraction of snow-free ground is obtained:

$$F_g = 100\,\frac{\sigma_i^0 - \sigma_w^0}{\sigma_g^0 - \sigma_w^0} \quad \% \tag{3}$$

where

- σ_i^0 observed backscattering coefficient during the snow melt period;
- σ_w^0 observed backscattering coefficient for wet snow at the beginning of the snow melt period;
- σ_g^0 observed backscattering coefficient for snow-free ground after the snow melt period.

In (3) the mean difference between the reference images ($\sigma_g^0 - \sigma_w^0$) is 3 dB or slightly less, depending on the land-use class. Due to the speckle in SAR images, it is advisable to average the σ^0 values of several pixels to increase the classification accuracy.

Using (3), two snow melt maps were produced, shown in Fig. 7. In the maps, solid red color indicates a high probability of snow melt and the more the color turns blue, the more the snow melt probability decreases. Solid blue color indicates that the area is covered by wet snow. Dark and gray pixels indicate areas where snow still covers about 50% of the ground. The snow melt map for May 5, 1993 suggests that snow has totally melted in few areas (red color). When these areas are compared with the land-use map (bottom left) these areas can be identified as agricultural land, open bog, and water. Also some darker values can be seen in bogs, on open areas, and at river banks which indicate that snow has partly melted in these areas. The map for May 20, 1992 shows a substantial progress in snow melt. Wet snow (blue color) exists only in densely forested areas. Snow in all open areas, bogs and water bodies has melted. The lakes do not show up well, because the backscattered power from calm water is low and, therefore, the difference between lake covered with wet snow and open lake is small. Based on snow melt maps in Fig. 7 and (3) a heuristic classification was performed to a subset of the test area (15 km $\times$ 13 km) including all test lines. The results of the classification are shown in Table IV. Although the test lines represented well the subset area geographically their video imagery covered only about 1% of the subset area. Tables III and IV show that within a single land-use class, the fraction of snow-free ground varied substantially between different test lines.

TABLE IV
SAR-BASED CLASSIFICATION OF SNOW-FREE GROUND FRACTION FOR DIFFERENT LAND-USE CLASSES. THE REFERENCE VALUES FOR MAY 5, 1993 ARE BASED ON VISUAL OBSERVATION MADE BY A HYDROLOGIST (TABLE III)

Land-use class	5 May 1993 Snow-free ground (%)		20 May 1992 Snow-free ground (%)
	SAR based estimate	visual observation	SAR based estimate
Agricultural land	42	9*	50
Gravel	37	76*	50
Clear-cut	34	9 - 70	68
Pine (0-50 m^3/ha)	22	9 - 31	68
Pine (50-100 m^3/ha)	20	5 - 21	42
Pine (100-150 m^3/ha)	18	1 - 31	40
Forested bog	25	12 - 43	90
All land-use classes	25		60

* Reference data is based only on one short test line

Verification of the above results is difficult because there were only five SAR images and they represent two different melting periods. Additionally, the airborne measurement cam-

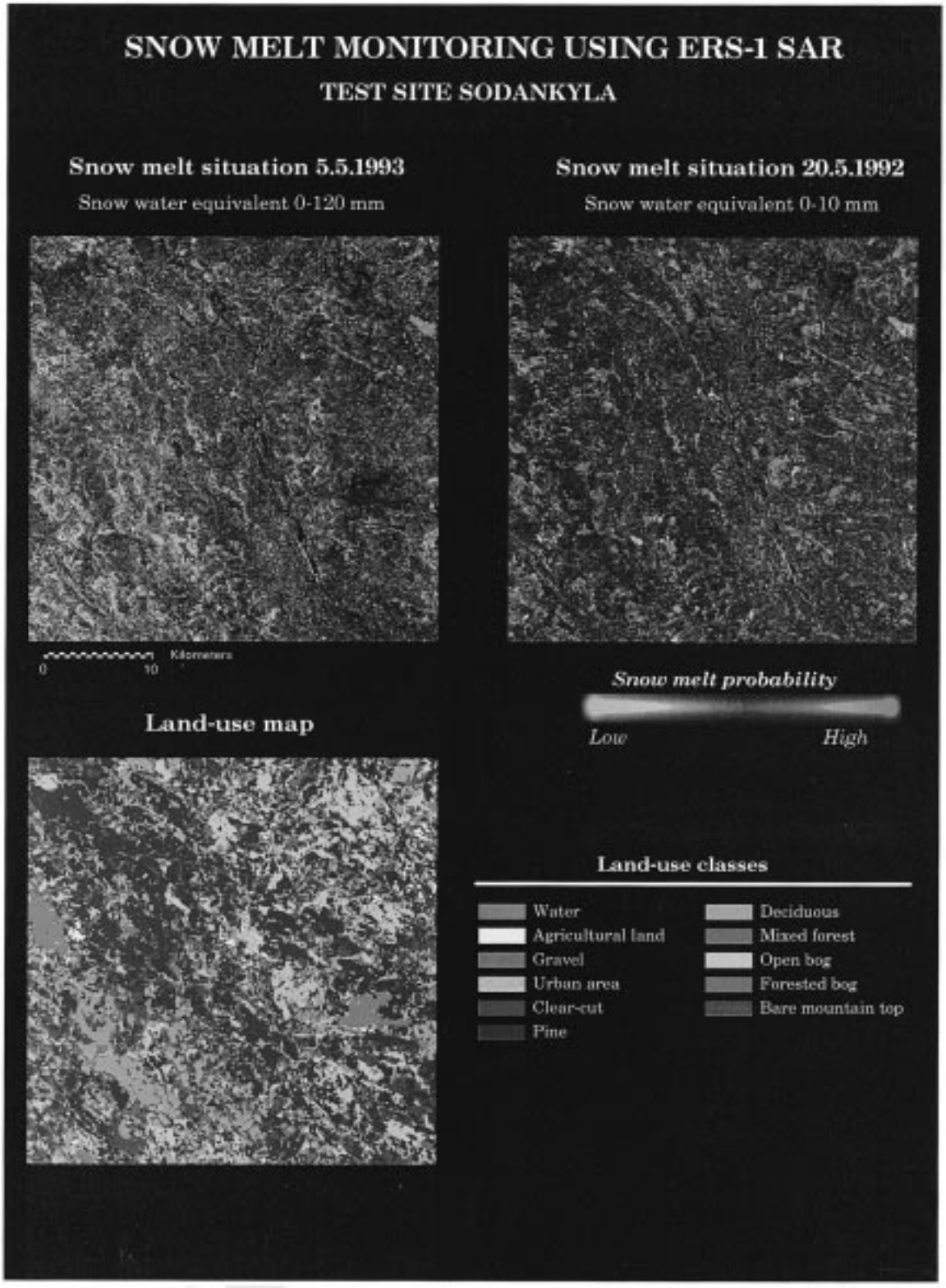

Fig. 7. Detection of snow melt by comparing a SAR image taken during the melt season with two SAR images acquired before and after the melt season. The snow melt probability bar is based on a maximum difference of 3 dB between the pixel-wise σ^0 values for snow-free ground and wet snow.

paign to monitor the snow melt was carried out only during the spring of 1993. Anyway, some viewpoints support the results obtained:

- In the snow melt maps derived from SAR images, snow melt is first detected in open areas which is in agreement with the general knowledge of the snow melt phenomenon,
- The snow melt results for different forest canopies are in agreement with the boreal forest semi-empirical model introduced in [23, [24], and

- The results from visual observation of snow-cover percentage in the test lines agree with the analysis made using the ERS-1 SAR images.

VII. Conclusions

Our results suggest that ERS-1 SAR has potential for snow-cover monitoring in the boreal forest zone. Although our results indicate that ERS-1 SAR cannot distinguish adequately dry snow and bare ground from each other, monitoring of snow melt progress is possible. The SAR is also sensitive to the biomass. In the case of a typical melting period, the correlation between the backscattering coefficient and the stem volume is higher than for other snow situations.

Based on this study,

1) wet snow can be distinguished from other soil/snow categories by using ERS-1 SAR;
2) the other categories (dry snow, dry ground, and wet ground) cannot be distinguished from each other with ERS-1 SAR;
3) progress in snow melt can be monitored by comparing SAR images taken during the melt season with two reference images (SAR images taken before and after the melt season). The reference images do not necessarily need to be acquired during the same melt season. Snow melt maps indicating the fraction of bare ground and melting (wet) snow can be derived from the comparison.

References

[1] M. Hallikainen, V. J¨a¨askeläinen, T. Häme, and J. Perälä, "Application of ERS-1 active microwave instrumentation data to remote sensing of snow," Helsinki Univ. Technol., Lab. Space Technol., Rep. 6, p. 34, 1992.

[2] A. Rango, "Effective use of satellite-observed snow cover data in the snowmelt-runoff model (SRM)," in *Proc. Workshop Applications of Remote Sensing in Hydrology*, Saskatoon, Sask., Canada, 1990, pp. 19–29.

[3] K. Seidel *et al.*, "Remote sensing of snow cover for operational forecasts," in *Proc. Int. Symp. Operationalization of Remote Sensing*, 1993, pp. 134–145.

[4] C. Mätzler, "Passive microwave signatures of landscapes in winter," *Meteorol. Atmosph. Phys.*, vol. 54, pp. 241–260, 1994.

[5] M. Hallikainen and P. Jolma, "Comparison of algorithms for retrieval of snow water equivalent from Nimbus-7 SSMR data in Finland," *IEEE Trans. Geosci. Remote Sensing*, vol. 30, pp. 124–131, Jan. 1992.

[6] H. Rott, "The analysis of backscattering properties from SAR data of mountain region," *IEEE J. Oceanic Eng.*, vol. 9, no. 5, 1984.

[7] J. Koskinen, L. Kurvonen, V. Jääskeläinen, and M. Hallikainen, "Capability of radar and microwave radiometer to classify snow types in forested areas," in *Proc. IGARSS'94 Symp.*, Pasadena, CA, 1994, pp. 1283–1286.

[8] T. Guneriussen, H. Johnsen, and K. Sand, "DEM corrected ERS-1 SAR data for snow monitoring," *Int. J. Remote Sensing*, vol. 17, no. 1, 1996.

[9] J. Shi, J. Dozier, and H. Rott, "Deriving snow liquid water content using C-band polarimetric SAR," in *Proc. IGARSS'93 Symp.*, Tokyo, Japan, 1993, pp. 1038–1041.

[10] M. Hallikainen, J. Hyyppä, J. Haapanen, T. Tares, P. Ahola, J. Pulliainen, and M. Toikka, "A helicopter-borne 8-channel ranging scatterometer for remote sensing, Part 1: Technical characteristics," *IEEE Trans. Geosci. Remote Sensing*, vol. 31, pp. 161–169, 1991.

[11] J. Perälä and M. Reuna, "The areal and time variability of snow water equivalent in Finland," National Board of Waters and Environment, Water, and Environment Research Inst., Hydrological Office (presently Finnish Environment Agency), ser. A 56, Helsinki, 1990, p. 260, in Finnish.

[12] E. Kuusisto, "Snow accumulation and snowmelt in Finland," Helsinki: Water Research Institute, 1984, no. 55.

[13] M. Uusitalo, "Yearbook of forest statistics 1988," *Folia Forestalia 730.* Helsinki: Finnish Forest Research Inst., 1989, p. 243.

[14] National Board of Waters and Environment, "Monthly hydrological report," National Board of Waters and Environment, Water, and Environment Research Inst., Hydrological Office (presently Finnish Environment Agency), no. 5, p. 6, 1992.

[15] M. Hallikainen, V. Jääskeläinen, J. Koskinen, T. Häme, and J. Perälä, "Application of ERS-1 SAR data to remote sensing of snow in Finland," in *Proc. IGARSS'92 Symp.*, Houston, TX, 1993, pp. 1661–1663.

[16] J. Paavilainen, T. Siltala, and A. Vertanen, "Digital land-use map, product specification," National Board of Survey, Dept. Remote Sensing, p. 1, 1992.

[17] E. Tomppo, "Finnish National Forest inventory," *Paper and Timber—The Mag. Finnish Forest Industries*, 1994, vols. 6 and 7, pp. 374–378.

[18] V. Jääskeläinen, "Remote sensing of snow with microwave radar," Licentiate thesis, Laboratory of Space Technol., Helsinki Univ. of Technology, Helsinki, Finland, p. 109, 1993, in Finnish.

[19] Y. Rauste, "Methods for analyzing SAR images," Rep. 612, Lab. Instrum. Technol., Technical Research Centre of Finland, Espoo, p. 99, 1989.

[20] H. Laur, "Derivation of backscattering coefficient σ^o in ERS-1.SAR.PRI products," European Space Agency, ESRIN, Iss. 1, Rev. 0, p. 16, 1992.

[21] J. Pulliainen, P. Mikkelä, M. Hallikainen, and J-P. Ikonen, "Seasonal dynamics of C-band backscatter of boreal forests with application to biomass and soil moisture estimation," *IEEE Trans. Geosci. Remote Sensing*, vol. 34, pp. 758–770, May 1996.

[22] C. W. Therrien, *Decision Estimation and Classification.* New York: Wiley, 1987, p. 251.

[23] J. Pulliainen, "Investigation on the backscattering properties of Finnish boreal forests at C- and X-band: A semi-empirical modeling approach," Ph.D. dissertation, Rep. 19, Lab. Space Technol., Helsinki Univ. of Technol., Espoo, p. 119, 1994.

[24] J. Pulliainen, K. Heiska, J. Hyyppä, and M. Hallikainen, "Backscattering properties of boreal forests at C- and X-band," *IEEE Trans. Geosci. Remote Sensing*, vol. 32, pp. 1041–1050, 1994.

[25] Y. Oh, K. Sarabandi, and F. Ulaby, "An empirical model and inversion technique for radar scattering from bare soil surfaces," *IEEE Trans. Geosci. Remote Sensing*, vol. 30, pp. 370–381, 1992.

[26] F. Ulaby, R. Moore, and A. Fung, *Microwave Remote Sensing, Active and Passive.* Reading: Addison Wesley, 1982, vol. II.

[27] E. Attema and F. Ulaby, "Vegetation modeled as water cloud," *Radio Sci.*, vol. 13, pp. 357–364, 1978.

[28] J. Piesbergen, F. Holecz, and H. Haefner, "Snow cover monitoring using multitemporal ERS-1 SAR data," in *Proc. IGARSS'95*, Florence, 1995, pp. 1750–1752.

Jarkko T. Koskinen (S'96) was born in Jyväskylä, Finland, in 1968. He received the M.Sc. degree from the Helsinki University of Technology (HUT) in 1994 and Licentiate of Technology degree in 1996, also from HUT. He is currently working toward the Doctor of Technology degree.

He is a research scientist in the Helsinki University of Technology, Laboratory of Space Technology. His research interests include active microwave remote sensing of snow and SAR interferometry.

Jouni T. Pulliainen (S'91–M'95), for a biography, see p. 404 of the March 1997 issue of this TRANSACTIONS.

Martti T. Hallikainen (M'83–SM'85–F'93), for a photograph and biography, see p. 377 of the March 1997 issue of this TRANSACTIONS.